Periodica Polytechnica
Civil Engineering

60(2), pp. 229–246, 2016
DOI: 10.3311/PPci.8222

RESEARCH ARTICLE

Optimal Design of Steel Towers Using a Multi-Metaheuristic Based Search Method

Ali Kaveh, *Vahid Reza* Kalatjari, *Mohammad Hosein* Talebpour

Received 12-05-2015, revised 02-07-2015, accepted 30-11-2015

Abstract

*In meta-heuristic algorithms, the problem of parameter tuning is one of the most important issues that can be highly time consuming. To overcome this difficulty, a number of researchers have improved the performance of their methods by enhancement and hybridization with other algorithms. In the present paper efforts are made to search design space simultaneously by the **M**ulti **M**etaheuristic based **S**earch **M**ethod (MMSM). In the proposed method, optimization process is performed by dividing the initial population into five subsets so-called islands. An improved multi-metaheuristic method is then employed. After a certain number of repetitions (migration intervals), some percent of the island's best members are transferred into another island (migration) and replaced by the members of low fitnesses. In the migration phase, the target island is chosen randomly. Examples of large design spaces are utilized to investigate the efficiency of the proposed method. For this purpose, steel are optimized utilizing the proposed method. The results indicate improvements in the available responses.*

Keywords

Multi Metaheuristic based Search Method (MMSM) · optimization · multi heuristic algorithms · power transmission towers

Ali Kaveh
Department of Civil Engineering, Iran University of Science and Technology, Tehran, Iran
e-mail: alikaveh@iust.ac.ir

Vahid Reza Kalatjari
Mohammad Hosein Talebpour
Department of Civil Engineering, Shahrood University of Technology, Shahrood, Iran

1 Introduction

Nowadays, optimization has attracted many researchers and engineers. An optimization process is supposed to lead to the best design fulfilling the existing limitations of the utilized code. In this regard, some factors consisting of the number of design variables, size of the search space and design controller constraints are amongst the barriers against achieving a minimum weight or cost design in an affordable computational time. This has led the researchers to develop different algorithms for optimal design of structures. There are two general categories of approaches for optimal design of structures. In the first category, optimization is performed based on mathematical programming methods. For the second category, optimization is based on random intelligent approaches taking advantages of probability theory as well as natural events. During the last decades, metaheuristic methods are considerably improved. These methods are mostly inspired by natural events. They search the total design space point by point and have the ability to work on every design space with every constraint, without limitations regarding the type of design variables. These properties have led the metaheuristic algorithms to be recognized as valuable tools to solve the optimization problems. The main idea of metaheuristic methods was first introduced by Fogle in 1966 through evolutionary strategy algorithm [1]. In 1975, Holland proposed Genetic algorithm-based optimization according to the structure of genes and chromosomes. The theory was developed by his students and Goldberg (1989) who proposed the present Genetic algorithm [2]. In 1983, Kirkpatrick presented an optimization method so-called simulated annealing which was based on the Metropolis computational algorithm according to gradual cooling theory [3]. Afterwards, in 1986 Glover proposed the tabu search optimization method [4]. Optimization method based on ant colonies was introduced by Dorigo [5]. In 1995, Eberhart and Kennedy [6] developed PSO method, inspired by birds and fish colony. Geem and et al. [7] suggested harmony search method according to musical process of searching for a perfect state of harmony. Then in 2006, Erol developed big bang-big crunch approach [8]. Two years later, gravitational search method based on physics laws exposed to discussion by Rashedi

[9]. In 2012, Kaveh and Talatahari [10] introduced the charged system search method based on physics laws and Newtonian mechanics. Finally, optimization method based on the behavior of ray passing through different layers of a media was presented by Kaveh and Khayatazad [11]. Some of the most recent metaheuristics can be found in a book by Kaveh [12].

In order to discuss and evaluate the advantages of the proposed methods, researchers tried to prove the efficiency through different benchmark examples so that a virtual competition has been recognized among the different metaheuristic algorithms for optimization of the structures. Being confident about the resulting response in an acceptable time has been the main criterion for this competition which led to different algorithms of different capabilities to optimize different structures. However, most of metaheuristic algorithms are faced with different inhibitors such as lack of information about values of the parameters, the probability of being trapped in a local optimum in the problems containing a large search space. This has led other researchers to offer suggestions to improve metaheuristic algorithms in order to obtain appropriate response in an acceptable time [12–14]. Some other researchers also tried to alleviate the disadvantages through incorporating different metaheuristic methods and derive benefits of the resulting hybrid algorithms [15–17]. In this regard, however, problems such as incorporating different metaeuristics and number of combinations, incorporating approaches, proposed methods for improving, etc. are among the most important factors to achieve the best results in optimal design of structures.

In the present paper, an attempt is made to employ several metaheuristic algorithms simultaneously through introducing MMSM in order to overcome some problems. In the MMSM, the initial population is divided into several small subsets called islands. Then a method based on each metaheuristic algorithm is allocated to each island, and the process is executed on each island. After several repetitions, using a migration process, the best designs from each island move among the islands and replace the low quality designs. According to the determined values of migration interval, this trend is continued until a predefined number of repetitions is completed [18–20]. In this way, dependency of the results on the relationships, parameters and the approach of each metaheuristic algorithm is considerably reduced. On the other hand, due to the parallel search in the design space this method has the ability of utilizing a parallel computing system. This capability can further increase the speed of the optimization and can lead to much better results in the design space. It is worth noting that for selecting suitable metaheuristic for each island, conventional metaheuristic algorithms are selected. Any other set of metaheuristic can be used in an MMSM approach. The presented recommendations try to increase the efficiency of each selected algorithm. In the present study two variants of MMSM denoted by MMSM 1 and MMSM 2 are employed for optimal design of steel towers. Since the search spaces of these structures are large, they are suitable candidates for evaluating the proposed algorithm. The results indicate good improvements in the optimal design of the studied examples.

2 The formulation of optmization process

The formulation of structural optimization can be expressed as follows:

Minimize

$$F(A) = \sum_{i=1}^{Ne} (\rho_i \ell_i a_i) \tag{1}$$

Subject to

$$C1: \sigma_j \leq \sigma_{all\,(Ten)}, |\sigma_j| \leq |\sigma_{all\,(Com)}| \quad j = 1, 2, \ldots, Ne \tag{2}$$

$$C2: |\Delta_k| \leq |\Delta_k^{max}| \quad k = 1, 2, \ldots, Ndof \tag{3}$$

In Eq. (1) the cross section design variables are defined in the form of a vector $[A]$ as follows:

$$[A] = [\alpha_1, \alpha_2, \ldots, \alpha_{Nos}]; \quad \alpha_i \in S; i = 1, \ldots, Nos \tag{4}$$

Parameters in Eqs. (1) to (4) are defined as follows:

ρ_i:	Materials density of each member.
l_i:	Length of each member.
a_i:	Cross-section of the *i*th member.
Ne:	Number of structure's members.
S:	List of the available profiles for design variables.
Nos:	Number of cross-sectional areas in each design.
σ_j:	Stress in the *j*th element of the structure.
σ_{all}:	Allowable compressive or tensile stress values.
Δ_k:	Nodal displacement of the *k*th degrees of freedom.
Δ_k^{max}:	Allowable displacement of the *k*th degrees of freedom.
Ndof:	Number of degrees of freedom of the active nodes.

Constraint C1: In structures like steel towers, the stresses due to the composition of load cases, should be in the allowable limits for all the members. This permissible amount is determined by codes [21–23]. Consequently, in the optimization process, the stress in each member is calculated and the value of constraint violation is determined according to the following:

$$C1 = \begin{cases} C_1^i = 0 \quad if \quad \left|\frac{\sigma_i}{\sigma_{all}}\right| - 1 \leq 0; i = 1, \ldots, Ne \\ C_1^i = \left|\frac{\sigma_i}{\sigma_{all}}\right| - 1 \quad if \quad \left|\frac{\sigma_i}{\sigma_{all}}\right| - 1 > 0; i = 1, \ldots, Ne \end{cases} \tag{5}$$

In this equation, the quantity of the constraint violation of the members is summed when the number of loading combinations is more than 1 and is equal to *nlc*.

Constraint C2: Performing structural analysis and calculating the stress values, if the displacements of the active nodes in every design is within the allowable range, then no penalty is assigned to the design. Otherwise, the constraint violation is determined as follows:

$$C2 = \begin{cases} C_2^i = 0 \;\; if \;\; \left|\frac{\Delta_i}{\Delta_i^{all}}\right| - 1 \leq 0; i = 1, \ldots, Ndof \\ C_2^i = \left|\frac{\Delta_i}{\Delta_i^{all}}\right| - 1 \;\; if \;\; \left|\frac{\Delta_i}{\Delta_i^{all}}\right| - 1 > 0; i = 1, \ldots, Ndof \end{cases} \tag{6}$$

In these equations, the constraint violations of the nodal displacements are summed when the number of load combinations is *nlc*.

3 Proposed optimization methods

Meta-heuristic algorithms are intelligent random search methods which search the design space by different points (different design). The logic of these algorithms is such that various enhanced designs are obtained during the optimization process. However, high number of parameters in some meta-heuristics and the lack of information about the suitable values of these parameters may cause trapping in local optimum. That is, finding suitable magnitudes for the parameters in each meta-heuristic method is one of the main difficulties of the metaheuristics. Many researchers have tried to improve metaheuristics by suggesting different solutions for this problem and also tried to decrease the impact of parameters of tuning of the algorithms [12–17].

In this paper, **M**ulti **M**etaheuristic based **S**earch **M**ethod (MMSM) is employed for optimal design of steel towers and power transmission towers. Reducing the effect of parameters of meta-heuristic algorithms and increasing the domain of search are two special features of this method. According to this method, initial population is divided to several islands. Each island has its own optimization method with distinct structure based on the associated meta-heuristic algorithm. This arrangement of action leads to variation in answers [18–20]. Here the proposed MMSM method is performed in two variants of MMSM 1 and MMSM 2, as shown in Fig. 1.

In MMSM 1 the initial populations are divided to 5 subpopulations, and improved metaheuristics comprising of GA, CSS, ACO, HS and PSO with different parameter values are utilized separately on the selected subpopulations. Each of these subpopulation are taken as an island. A number of the best designs (migration number) of each island are selected after a number of iteration and moved alternately to the islands. This process is shown in Fig. 1(a). In the process of migration the following two parameters play important roles:

Migration interval which is the same as the number of iterations in each migration.

Migration rate that is the number of selected designs (in the form of percentage) to migrate from each island to the other island in migration intervals.

In the process of migration each subpopulations have a random destination which becomes known in each period of migration. A migration sends some of the best designs of a subpopulation to another island which has different context and structure. After completion of the process of migration, the migrated members together with the remaining members of that island form a new population and the optimization is further performed for obtaining better designs. Die to the migration process, in the MMSM 1the results have diverse properties. This is because of the properties of each island and all the incorporated metaheuristics play active role. In other words optimization is performed by simultaneous use of different metaheuristics and the method attempts to increase the quality o f the results by providing enhanced members. Fig. 2 show the optimization process based on the MMSM 1.

Similar to MMSM 1, in MMSM 2 the initial populations are divided to 5 subpopulations, and improved metaheuristics comprising of GA, CSS, ACO, HS and PSO with different parameter values are separately utilized for each island. Then the best island is selected based on the smallest mean value of the sum of the objective function (Eq. (1)) and penalty function (Eq. (3))

$$F_{merit} = F_{Penalty} + F(A) \tag{7}$$

Then the best designs of the islands are migrated to the best island. Ultimately the optimization process is performed on the best island based on the corresponding metaheuristic until the termination criterion is fulfilled. In MMSM 2 migration interval and migration rate can be defined as follows:

Migration interval is the number of iterations performed before the migration process starts.

Migration rate is the number of members selected for migration (in the form of percentage) for migration to the best island.

In MMSM 2, each problem is optimized with different metheuristic algorithms and the search space is explored, until all good designs are collected in the best island and from then on the optimization is carried out by the metaheuristic of the best island. Migration interval in this method is more than MMSM 1. Fig. 3 illustrates the optimization process based on this method.

In problems like steel power transmission towers where the size of the search space leads to substantial effect of each metaheuristic method in the optimization process, using MMSM, the design space is explored more effectively and thus better results are obtained. Stable state of MMSM methods results in the tendency of the optimization algorithm to find global optimum.

3.1 Island (1)

In this article, optimization of island (1) is performed based on the Genetic Algorithm (GA). This optimization process is performed in the following steps [2, 18]:

First, an initial population is randomly formed with binary characters. Then, the value of the objective function and the constraint violations are determined. In this article, the proposed penalty function with dynamic features is used which has a good

Fig. 1. Two MMSMs of the Multi Metaheuristic based Search Method

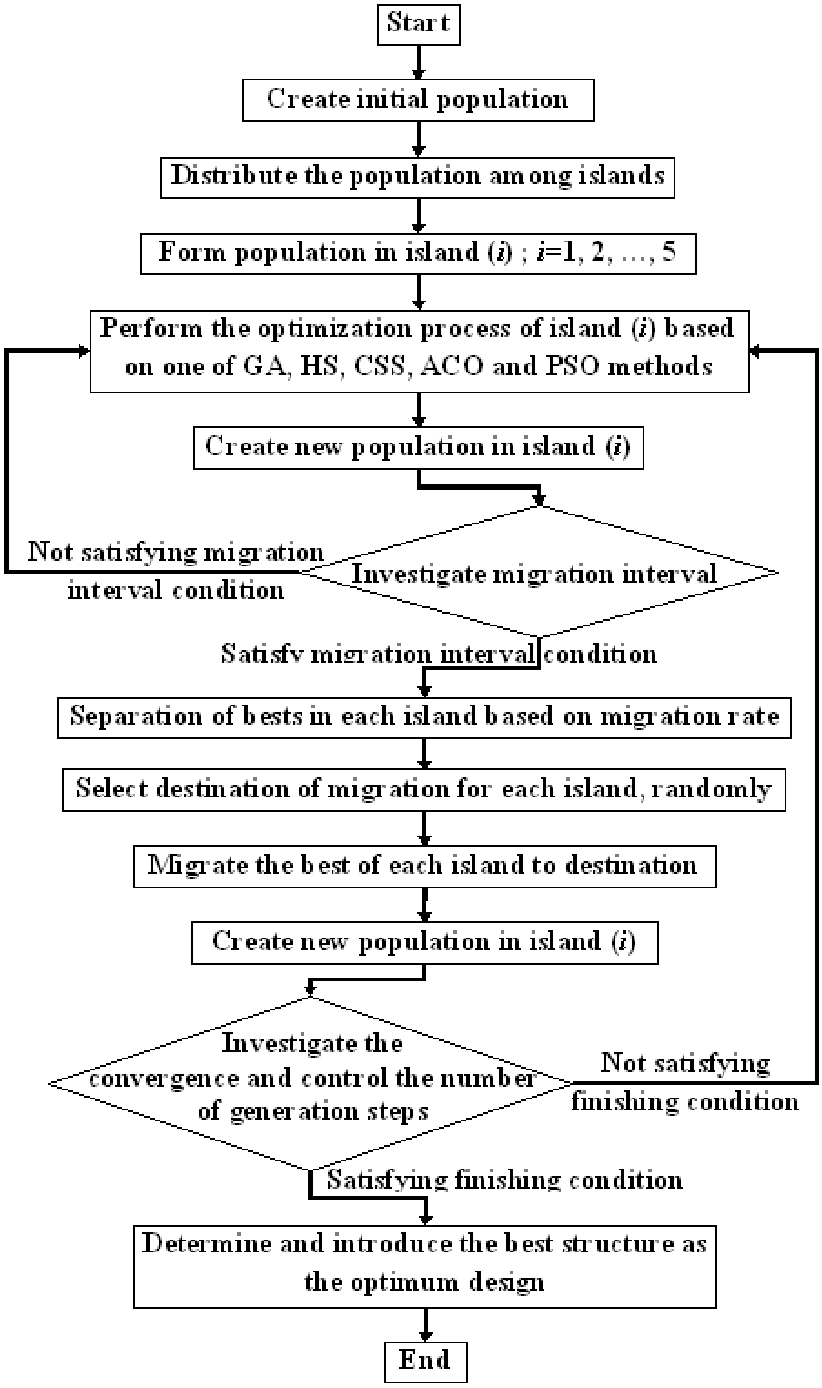

Fig. 2. First variant of the Multi Metaheuristic Searching Method (MMSM 1)

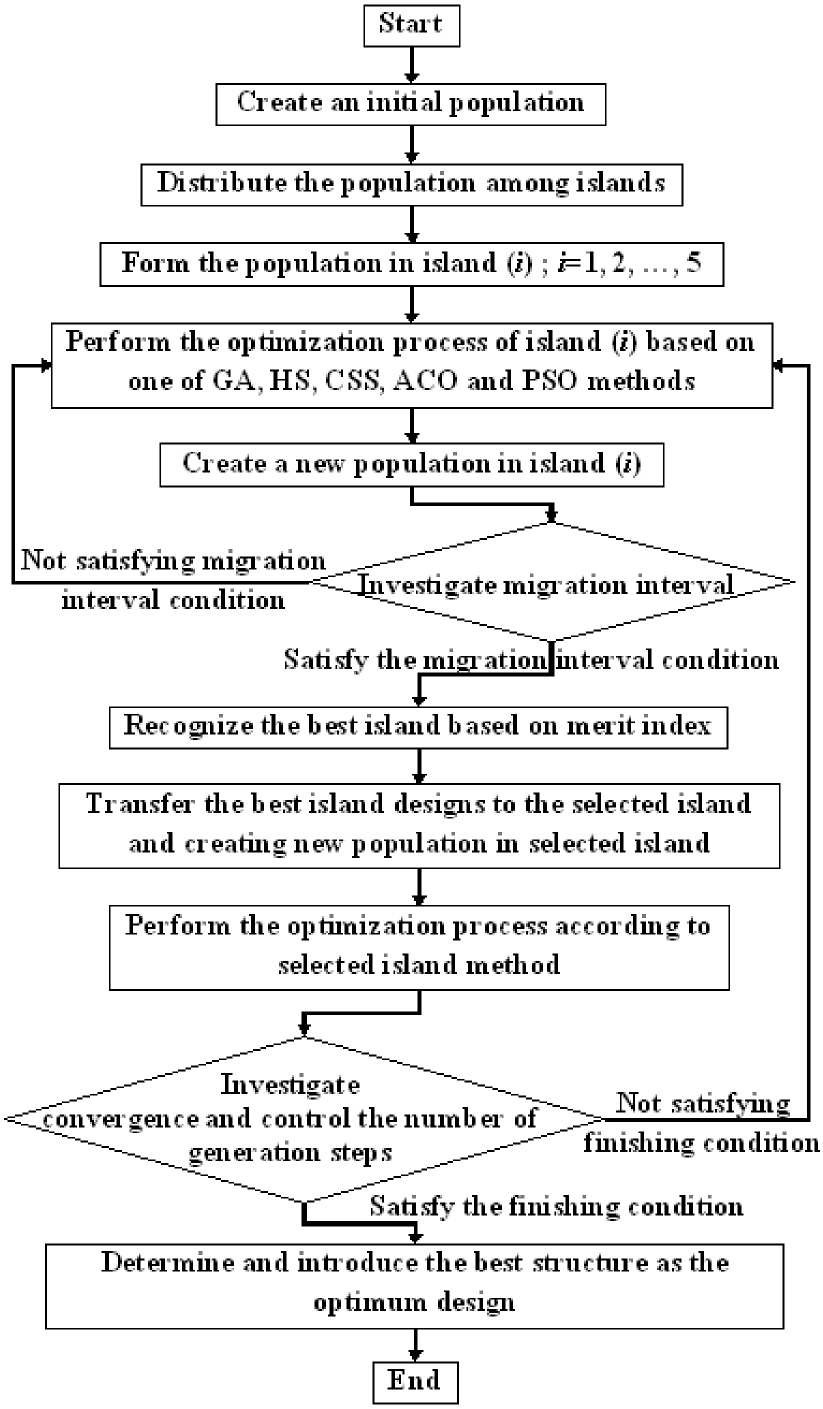

Fig. 3. Second variant of the Multi Metaheuristic Searching Method (MMSM 2)

compatibility with the algorithms of the MMSM.

$$f_{penalty} = F(A).K.C_g$$
$$C_g = \sum^{nlc} \sum_{q=1}^{4} \max\left[0, g_{iq}(A)\right] \quad (8)$$
$$K = k_j \times Ln(j+1)\,;\, j = 1, ...nk$$

In this equations, $g_{iq}(A)$ is the characteristic of the constraint violation, and C_g is the representative of the sum of all violations that has occurred by the structure in order to resist all the load combinations of the *nlc*. K is the constant of dynamic penalty, k_j is a constant quantity of each migration range for total number of *nk*, and j is the counter of each migration interval. Afterwards, the merit of each design is computed based on the objective function and the proposed penalty function [24].

Then, the best designs are selected using a replication process that is inspired by natural development rules. In this island, tournament method [18] is used for the selection process. Once the selection process is completed, the crossover operator is applied in order to produce a population of offsprings. For this purpose, uniform crossover is used with small changes [18]. Therefore, parent's strings are selected based on the crossover rate. Then, a string which is called mask, is randomly produced. This string consists of binary bits as length of each string. In the next step, a uniform random number is produced for each bit and is compared to the amounts resulted from Eq. (9). Offspring's bits is selected based on the mask pattern if the random number become more than the amount obtained by Eq. (9). That is, if the amount of the bit in the mask is equal to one, the bit of the first offspring will be from the first parent, otherwise, it is selected from the second parent. Although, while the randomly produced number is less than the amount obtained from Eq. (8), the bit of the offspring's strings are selected from more meritorious parent.

$$P_{C2} = P_{C2}^{Min} + \left(P_{C2}^{Max} - P_{C2}^{Min}\right)\frac{t}{T} \quad (9)$$

Where P_{C2} is the secondary rate of crossover in each generation for each bit, P_{C2}^{Max} and P_{C2}^{Min} are respectively the maximum and the minimum rate of the secondary crossover in the optimization process (based on the input of the user), t is the number of current generation, and T is the total number of generations. In this article, a method is proposed which is used dynamically to apply the mutation operator. Thus, first the total number of making generations is divided into a number of bits of each substring in design variable and several intervals are formed. Then, the common operator of the mutation is applied to all the bits in each substring. After performing this process in the first interval, the first bit at the left-side of each substring becomes stabilized, and the rate of the mutation probability for it will be equal to zero, and the optimization process will be continued till the end of the second interval of the total number of making generations. Afterwards, the mutation rate of the two bits at the left-side becomes zero and this process is continued until the last bit in the substring. It should be mentioned that the rate of the mutation probability for the residual bits in each interval is performed utilizing the following equation [18]:

$$P_m = P_m^{Max} - \left(P_m^{Max} - P_m^{Min}\right)\frac{t}{T} \quad (10)$$

In which P_m is the mutation rate in each interval, $P_m^{Max}$and P_m^{Min} are, respectively, the maximum and minimum amount of mutation rate in optimization process (based on the input of the user), t is the number of present interval and T is the number of all intervals.

3.2 Island (2)

In island (2), the Harmony Search (HS) algorithm is used [7, 24, 25]. According to this algorithm, in the process of optimization each musician substitute with design variable and collection of musician make the vector of design variable. Quality of music is substituted by the value of the object function. Optimization process for this algorithm is performed as follows:

First, HS parameters such as $HMCR$, PAR, HMS, etc. are initialized. Then, the initial population (HM) based on HMS (number of population members in island (2)) is randomly formed as a matrix.

$$HM = \begin{bmatrix} x_1^1 & x_2^1 & \dots & x_N^1 \\ x_1^2 & x_2^2 & \dots & x_N^2 \\ \vdots & \vdots & & \\ x_1^{HMS} & x_2^{HMS} & \dots & x_N^{HMS} \end{bmatrix}_{HMS\times N} \quad (11)$$

In MMSM for the current island in spite of general process of HS [25], initial population with no constraint violation is not required and fitness of each design is specified on the basis of constraint violation and objective function. In order to compute the amount of fitness for each design, the proposed penalty function is used according to Eq. (8).

Optimization process is continued for HM by producing a new member based on the HS rules. Vectors of the new design variables $X\prime = [x_1\prime, x_2\prime, \dots, x_N\prime]$ are made by three possible variants of HS rules and $HMCR$ and PAR parameters. Accordingly, each amount of $x_1\prime$ can be randomly produced again, or can be determined by the existing corresponding amounts in HM. This step is performed by producing a uniform random number between zero and one, and comparing it with the amount of $HMCR$. If the random number is more than $HMCR$, $x_i\prime$ is determined randomly and based on variable range, otherwise, the amount of $x_i\prime$ is settled by HM. Determination of $x_i\prime$ in HM is by PAR parameter. Therefore, a uniform random number between zero and one is produced and by comparing it with the value of PAR, $x_i\prime$ is defined. If the random number is less than PAR, $x_i\prime$ will be selected from the existing corresponding value of the HM. Otherwise,$x_i\prime$ is determined based on the value of the bw and from neighborhood of corresponding values with$x_i\prime$

at HM. Finally, if the vector of design variable is better than worst vector in HM, then the new vector will replace the worst vector. Otherwise, HM remains unaltered.

This article suggests that PAR and bw parameters should change based on the amount of migration of the interval as follow:

$$PAR = PAR_{\min} + \frac{(PAR_{\max} - PAR_{\min})}{nk} \times j \quad j = 1, ...nk \tag{12}$$

$$bw = bw_{\max} \times \exp\left(\frac{\ln(bw_{\min}/bw_{\max})}{nk} \times j\right) \quad j = 1, ...nk \tag{13}$$

Where, the indices max and min refer to the maximum and minimum values of the related parameter. j and nk are the number of migration interval and total number of migration interval in the optimization process, respectively. Migration interval, based on the amount of PAR and bw parameters, has different values that ascends for PAR and exponentially descends for bw during the entire process of the optimization. Varying these parameters has valuable influence on the optimization process.

3.3 Island (3)

The Charged System Search (CSS) method is used to perform optimization process [10]. In the CSS method, optimization process is performed based on the charged particles laws and Newton laws of motion. Thus, each vector of design variables is considered as a charged particle which possesses electric field as a result of electric charge. Each particle is affected by the electric field of the other particles and proportional to the amount of electric force of other particles and Newton laws of motion, the particle moves in design space to a new position. The optimization process is performed as follows [26]:

First, similar to other meta-heuristic methods the initial population is randomly produced and other parameters of the CSS method such as the number of particles, number of selected particles of CMS and so on are initialized. Then, the fitness of each particle is computed according to value of the object function and the proposed penalty function in Eq. (7). The magnitude of the charge of each particle (q_s) and motion probability of particle of s affected by the force of the rth particle, P_{rs} , is obtained by the following equation:

$$q_s = \frac{fit_s - fit_{worst}}{fit_{best} - fit_{worst}} \quad s = 1, \ldots, \text{Charge Size} \tag{14}$$

$$P_{rs} = \begin{cases} 1 & \frac{fit_r - fit_{best}}{fit_s - fit_r} > ran \vee fit_s > fit_r \\ 0 & else \end{cases} \tag{15}$$

fit_{best} and fit_{worst} are fitnesses of the best and the worst existing design in current population, respectively. A small population which consists of the bests of the existing population is called CMS is produced after computing the p_{rs} and q_s. Then, the resultant electrical force acting on a particle is computed using the following equation:

$$F_s = q_s \sum_{r, r \neq s} \frac{q_r}{a^3} r_{rs} P_{rs} (X_r - X_s) \quad if \ \ r_{rs} < a \tag{16}$$

$$F_s = q_s \sum_{r, r \neq s} \frac{q_r}{r_{rs}^2} P_{rs} (X_r - X_s) \quad if \ \ r_{rs} \geq a \tag{17}$$

Where a is the diameter of each particle, r_{rs} is the distance between two particles r and s that is defined according to position of the particles X_r and X_s. New position of each particle in the design space is determined by the following equation:

$$X_{s,new} = X_{s,old} + r_1 k_a F_s + r_2 k_v v_{s,old} \tag{18}$$

$$v_{s,new} = X_{s,new} - X_{s,old} \tag{19}$$

r_1 and r_2 are uniform random numbers between zero and one. v_s is also the velocity of the particle s, k_a and k_v are respectively, the velocity and acceleration coefficients which are computed to associate with MMSM as:

$$k_a = 0.5\,(1 + j/nk)\,; \quad j = 1, ...nk \tag{20}$$

$$k_v = 0.5\,(1 - j/nk)\,; \quad j = 1, ...nk \tag{21}$$

New position of each particle is assessed during the optimization process, providing the amount of exiting from the allowable range. Design variables are then modified based on the HS method and CMS population [26].

3.4 Island (4)

Ant Colony Optimization (ACO) is used in island (4) [5]. This algorithm is executed by the following steps [24, 27]:

First, the amount of initial pheromone is specified. In order to calculating fit_0, the first cross-section area in the profile list is initialized for design variables, and then the initial pheromone is determined according to following equation:

$$\tau_0 = \frac{1}{fit_0} \tag{22}$$

Then, the probability of selection is evaluated based on the following equation [27]:

$$p_{ij} = \frac{\tau_{ij}^{\alpha} \upsilon_i^{\beta}}{\sum\limits_{k=1}^{N} \tau_{kj}^{\alpha} \upsilon_k^{\beta}} \tag{23}$$

Where, τ_{ij} is the amount of existing pheromone in the ith path (state number i for the considered design variable) for the design variable number j, and N is the number of possible states for the considered design variable. υ_i is also calculated by Eq. (24) for each design variable.

$$\upsilon_i = \frac{1}{A_i} \tag{24}$$

A_i refers to the selected cross-section area of the ith path. The amount of the variable number i is determined by p_{ij} similar to the tournament method in GA. After determining the amount of all the design variables, the amount of the pheromone in the selected path is determined as follows:

$$\tau_{ij}^{new} = \rho.\tau_{ij}^{old} \tag{25}$$

Where ρ is the local update parameter to which a suitable value between zero and one is assigned.

Then, the amount of fitness is calculated and existing population designs are sorted [27]. Pheromone evaporation process for all the possible paths is done based on the following equation:

$$\tau_{ij}^{new} = (1 - e_r).\tau_{ij}^{old} \tag{26}$$

Where, e_r is a constant referred to as the evaporation rate. After evaporation of pheromone, the process of depositing pheromone in the selected paths is executed as follow:

$$\tau_{ij} = \tau_{ij} + e_r.\left[\left(\Delta\tau_{ij}\right) + \sum_{k=1}^{\lambda_r} (\lambda_r - k)\left(\Delta\tau_{ij}\right)_k\right] \tag{27}$$

In the above equation, λ_r is number of the best existing population and k is the number of considered design in small population of the bests.$\left(\Delta\tau_{ij}\right)_k$ in Eq. (27) is calculated for ant number k by the following equation:

$$\left(\Delta\tau_{ij}\right)_k = \frac{1}{fit_k} \tag{28}$$

3.5 Island (5)

Particle Swarm Optimization (PSO) is used in island (5) [6, 24]. This algorithm is influenced by the social behaviour of the birds in searching food. The PSO algorithm begins by producing an initial random population. Particle number i (design) which introduces bird number i in the group of birds is defined by two variables $X_i = [x_{i1}, x_{i2}, ..., x_{iN}]$ and $V_i = [v_{i1}, v_{i2}, ..., v_{iN}]$. X_i is the position and V_i is velocity of the particle number i in the search space. In each step of group movement (repeat), particle position is changed by two amounts of $P_{best,i}$ and R_{best}. The position of each particle (design) is determined in the search space utilizing the following equations:

$$X_i^{k+1} = X_i^k + V_i^{k+1} \tag{29}$$

$$V_i^{k+1} = \omega V_i^k + c_1 r_1 \left(p_{best,i}^k - X_i^k\right) + c_2 r_2 \left(R_{best}^k - X_i^k\right) \tag{30}$$

In the above equation, X_i^k is the position of the ith particle in the kth iteration, V_i^k is velocity of the ith particle in the kth iteration, ω is the inertia weight in the previous step, r_1 and r_2 are the uniform random numbers between zero and one, C_1 and C_2 are the acceleration constants. $P_{best,i}^k$ is the best position of the particle i from first to iteration number k, R_{best}^k is the best position of a particle from the first to iteration number k among all the particles.

In this article, the amount of variable velocity of the particles is controlled by defining minimum and maximum velocity (v_{min} , v_{max}). In this regard,v_{min} and v_{max}, based on the coefficient of maximum and minimum amount of x are defined. In order to be compatible with the MMSM, the parameter ω is changed based on the number of migration interval as:

$$\omega = \omega_{\max} - \frac{(\omega_{\max} - \omega_{\min})}{nk} \times j; \quad j = 1, ...nk \tag{31}$$

ω_{max} and ω_{min} are the maximum and minimum value of ω, respectively. j and nk are the number and total number of migration interval in the optimization process, respectively. Therefore, the value of ω is linearly altered in each migration, with initial amount of ω_{max} and final amount of ω_{min}. This method in altering the ω resulting in a balance between the local and global search in the PSO algorithm.

4 Numerical examples

In order to evaluate the capability of MMSM algorithm, typical examples of the optimization of power transmission towers and steel towers, are considered and the results are compared to the results of other references. The results indicate that the MMSM explores the search space more accurately than the other existing methods and provides better results.

4.1 A 582-bar steel tower

A 582-bar steel tower with the height of 80 m, shown in Fig. 4, is chosen from [15, 24] as the first example. According to the symmetry of the structure with respect to x-axis and y-axis, the structural members are categorized into 32 groups.

A single load case is considered consisting of lateral loads of 5 kN (1.12 $kips$) applied in both x- and y- directions and a vertical load of -30 kN (-6.74 $kips$) applied in the z-directions in all the nodes of the tower. A discrete set of 137 economical standard steel sections selected from W-shape profile list based on the area and radius of gyration properties is used to size the variables [15, 24]. The lower and the upper bounds on size variables are taken as 6.16 in^2 (39.74 cm^2) and 215 in^2 (1387.09 cm^2), respectively.

The allowable tensile and compressive stresses are considered according to the provisions of ASD-AISC [23] and the allowable compressive stress is defined as follows:

When $\lambda < C_c$:

$$\sigma_{all(com)} = \left(F_y\left[1 - \frac{\lambda^2}{2C_c^2}\right]\right) / \left(\frac{5}{3} + \frac{3\lambda}{8C_c} - \frac{\lambda^3}{8C_c}\right) \tag{32}$$

and when $\lambda \geq C_c$:

$$\sigma_{all(com)} = \frac{12\pi^2 E}{23\lambda^2} \tag{33}$$

Where E is the modulus of elasticity and F_y is the yield stress of steel which are considered as 203893.6 MPa (29000 ksi) and 253.1 MPa (36 ksi), respectively. λ is the maximum slenderness

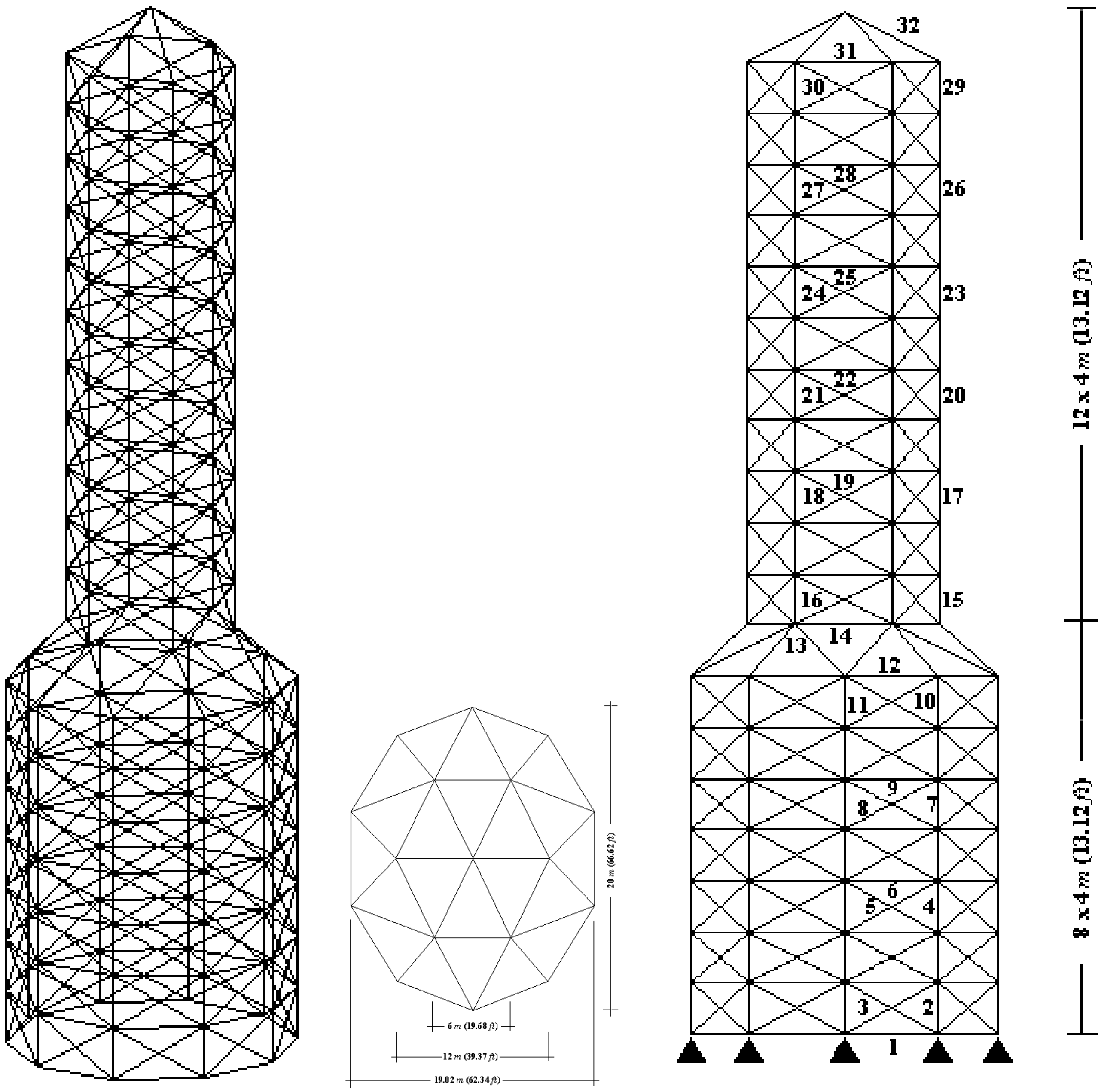

(a) (b) (c)

Fig. 4. Schematic of a 582-bar steel tower

ratio and for the compressive members in x- and y- directions is calculated as follows:

$$\lambda = l/r_i; \quad i = x, y \tag{34}$$

Where l is the length of the member and r_i is the radius of gyration of the section.

In Eq. (35), C_c is the slenderness ratio dividing the elastic and inelastic buckling regions, which is calculated as follow:

$$C_c = \sqrt{\frac{2\pi^2 E}{F_y}} \tag{35}$$

The allowable tensile stress based on provisions of ASD-AISC [23] is estimated as follows:

$$\sigma_{all(Ten)} = 0.6F_y \tag{36}$$

The maximum slenderness ratio is limited to 200 for compression members, and it is recommended to be 300 for tension members according to ASD-AISC design code provision [23]. In addition, the displacements of all nodes are limited to 8 *cm* (3.15 *in*) in each direction.

Following the optimization process based on the MMSM, the trend is obtained as shown in Fig. 5, where the diagram of average of 10 independence and consecutive performances of optimization process are plotted. It is evident that the graph of the best state and the average of consecutive performances are very close indicating the relative independence of the MMSM from the existing parameters in the algorithm of islands. In other words, based on MMSM, the effect of the parameters for every available method in islands is decreased. On the other hand, diagram proximity of the best performance and average of consecutive performances indicate the reliability of the MMSM in obtaining the optimum design.

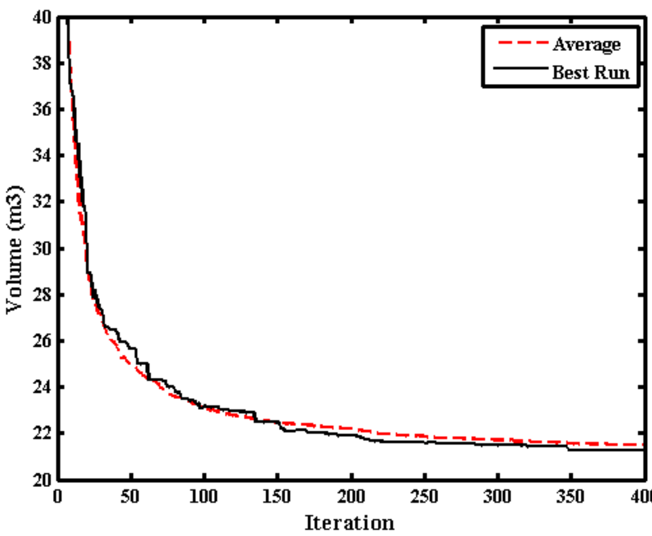

Fig. 5. The convergence history of the 582-bar steel tower

The comparison between MMSM and other references is summarized in Table 1. As it can be seen, the resulting design based on MMSM is lighter than the other sources. Accordingly, MMSM explores the design space more accurately and regarding the weight, presents more lighter design in comparison to other references.

4.2 A 244-bar power transmission tower

In this example, the 244-bar power transmission tower, shown in Fig. 6, is investigated.

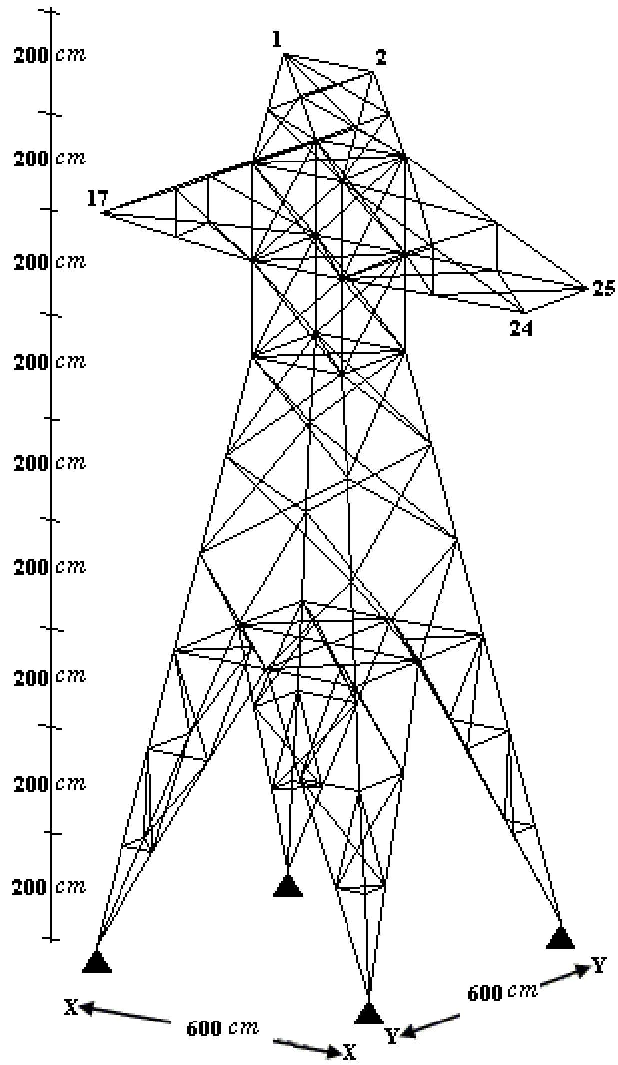

Fig. 6. Schematic of a 244-bar power transmission tower

Members of structure are categorized into 26 groups and the effective loads on the structure are considered for two conditions (Table 2).

A discrete set for design process is listed in Table 3. Values of the allowable tensile and compressive stresses are calculated using Eqs. (31), (32) and (35) based on ASD-AISC code [23]. In this example, E and F_y are assumed to be 210 kN/mm^2 and 233.3 N/mm^2, respectively [28]. The allowable tensile stress is taken as 140 N/mm^2.

In this example, the maximum slenderness ratio is limited to 200 for compression members, and it is recommended to be limited to 300 for tension members [23]. In addition, the nodal displacement constraints for the 244-bar tower are defined in

Tab. 1. Optimal design comparison for the 582-bar steel tower

Element group	Hasançebi et al. [24]	Kaveh et al. [15]	This study
	PSO	DHPSACO	MMSM
1	W8 x 21	W8 x 24	W8 x 21
2	W12 x 79	W12 x 72	W12 x 72
3	W8 x 24	W8 x 28	W8 x 28
4	W10 x 60	W12 x 58	W10 x 54
5	W8 x 24	W8 x 24	W8 x 24
6	W8 x 21	W8 x 24	W8 x 21
7	W8 x 48	W10 x 49	W10 x 49
8	W8 x 24	W8 x 24	W8 x 24
9	W8 x 21	W8 x 24	W8 x 21
10	W10 x 45	W12 x 40	W8 x 40
11	W8 x 24	W12 x 30	W8 x 24
12	W10 x 68	W12 x 72	W12 x 72
13	W14 x 74	W18 x 76	W18 x 76
14	W8 x 48	W10 x 49	W10 x 49
15	W18 x 76	W14 x 82	W14 x 82
16	W8 x 31	W8 x 31	W8 x 31
17	W8 x 21	W14 x 61	W21 x 62
18	W16 x 67	W8 x 24	W8 x 24
19	W8 x 24	W8 x 21	W8 x 21
20	W8 x 21	W12 x 40	W8 x 40
21	W8 x 40	W8 x 24	W8 x 24
22	W8 x 24	W14 x 22	W8 x 21
23	W8 x 21	W8 x 31	W12 x 26
24	W10 x 22	W8 x 28	W8 x 24
25	W8 x 24	W8 x 21	W8 x 21
26	W8 x 21	W8 x 21	W8 x 21
27	W8 x 21	W8 x 24	W8 x 24
28	W8 x 24	W8 x 28	W8 x 21
29	W8 x 21	W16 x 36	W8 x 21
30	W8 x 21	W8 x 24	W8 x 24
31	W8 x 24	W8 x 21	W8 x 21
32	W8 x 24	W8 x 24	W8 x 24
Volume in^3 (m^3)	**1366674.89 (22.3958)**	**1346227.65 (22.0607)**	**129596.16 (21.2373)**

Tab. 2. The load cases and displacement bounds for the 244-bar power transmission tower

Loading conditions	Joint number	Loads (*kN*)		Displacement limitations (*mm*)	
		X	Z	X	Z
1	1	10	−30	45	15
	2	10	−30	45	15
	17	35	−90	30	15
	24	175	−45	30	15
	25	175	−45	30	15
2	1	–	−360	45	15
	2	–	−360	45	15
	17	–	−180	30	15
	24	–	−90	30	15
	25	–	−90	30	15

Tab. 3. Available cross-sections for the 244-bar power transmission tower

No.	Section	A - in^2 (mm^2)	r - in (mm)	No.	Section	A - in^2 (mm^2)	r - in (mm)
1	L 6 x 6 x 1	11.0 (7096.76)	1.17 (29.72)	24	L 3 1/2 x 3 1/2 x 1/2	3.25 (2096.77)	0.683 (17.35)
2	L 6 x 6 x 7/8	9.73 (6277.41)	1.17 (29.72)	25	L 3 1/2 x 3 1/2 x 7/16	2.87 (1851.61)	0.684 (17.37)
3	L 6 x 6 x 3/4	8.44 (5445.15)	1.17 (29.72)	26	L 3 1/2 x 3 1/2 x 3/8	2.48 (1600.00)	0.687 (17.45)
4	L 6 x 6 x 5/8	7.11 (4587.09)	1.18 (29.97)	27	L 3 1/2 x 3 1/2 x 5/16	2.09 (1348.38)	0.690 (17.53)
5	L 6 x 6 x 9/16	6.43 (4148.38)	1.18 (29.97)	28	L 3 1/2 x 3 1/2 x 1/4	1.69 (1090.32)	0.694 (17.63)
6	L 6 x 6 x 1/2	5.75 (3709.67)	1.18 (29.97)	29	L 3 x 3 x 1/2	2.75 (1774.19)	0.584 (14.83)
7	L 6 x 6 x 7/16	5.06 (3264.51)	1.19 (30.23)	30	L 3 x 3 x 7/16	2.43 (1567.74)	0.585 (14.86)
8	L 6 x 6 x 3/8	4.36 (2812.90)	1.19 (30.23)	31	L 3 x 3 x 3/8	2.11 (1361.29)	0.587 (14.91)
9	L 6 x 6 x 5/16	3.65 (2354.83)	1.20 (30.48)	32	L 3 x 3 x 5/16	1.78 (1148.38)	0.589 (14.96)
10	L 5 x 5 x 7/8	7.98 (5148.38)	0.973 (24.71)	33	L 3 x 3 x 1/4	1.44 (929.03)	0.592 (15.04)
11	L 5 x 5 x 3/4	6.94 (4477.41)	0.975 (24.77)	34	L 3 x 3 x 3/16	1.09 (703.22)	0.596 (15.14)
12	L 5 x 5 x 5/8	5.86 (3780.64)	0.978 (24.84)	35	L 2 1/2 x 2 1/2 x 1/2	2.25 (1451.61)	0.487 (12.37)
13	L 5 x 5 x 1/2	4.75 (3064.51)	0.983 (24.97)	36	L 2 1/2 x 2 1/2 x 3/8	1.73 (1116.13)	0.487 (12.37)
14	L 5 x 5 x 7/16	4.18 (2696.77)	0.986 (25.04)	37	L 2 1/2 x 2 1/2 x 5/16	1.46 (941.93)	0.489 (12.42)
15	L 5 x 5 x 3/8	3.61 (2329.03)	0.990 (25.15)	38	L 2 1/2 x 2 1/2 x 1/4	1.19 (767.74)	0.491 (12.47)
16	L 5 x 5 x 5/16	3.03 (1954.83)	0.944 (25.25)	39	L 2 1/2 x 2 1/2 x 3/16	0.902 (581.93)	0.495 (12.57)
17	L 4 x 4 x 3/4	5.44 (3509.67)	0.778 (19.76)	40	L 2 x 2 x 3/8	1.36 (877.42)	0.389 (9.88)
18	L 4 x 4 x 5/8	4.61 (2974.19)	0.779 (19.79)	41	L 2 x 2 x 5/16	1.15 (741.93)	0.390 (9.91)
19	L 4 x 4 x 1/2	3.75 (2419.35)	0.782 (19.86)	42	L 2 x 2 x 1/4	0.938 (605.16)	0.391 (9.93)
20	L 4 x 4 x 7/16	3.31 (2135.48)	0.785 (19.94)	43	L 2 x 2 x 3/16	0.715 (461.29)	0.394 (10.00)
21	L 4 x 4 x 3/8	2.86 (1845.16)	0.788 (20.02)	44	L 2 x 2 x 1/8	0.484 (312.26)	0.398 (10.11)
22	L 4 x 4 x 5/16	2.40 (1548.38)	0.791 (20.09)	45	L 1 1/4 x 1 1/4 x 3/16	0.434 (280.00)	0.244 (6.198)
23	L 4 x 4 x 1/4	1.94 (1251.61)	0.795 (20.19)				

Table 2.

Fig. 7 shows the convergence trend of the average consecutive runs and the best run based on the MMSM for the 244-bar power transmission tower. As demonstrated, average graph trend and the best performance graph are close to each other which shows constant and stable trend in optimization process of the MMSM in obtaining minimum and relative dependence of the proposed method to parameters in comparison to heuristic algorithm. On the other hand, proximity of the average graph and best performance graph indicate relative independence of MMSM from consecutive performances in obtaining acceptable response.

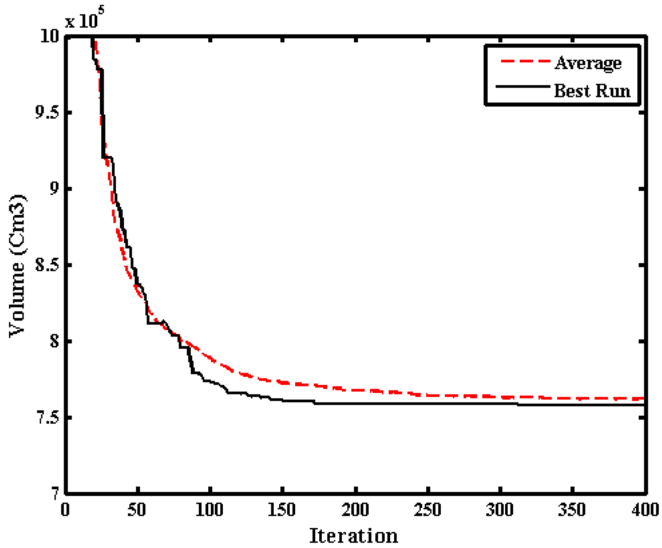

Fig. 7. The convergence history for the 244-bar power transmission tower

Results of using MMSM are presented in Table 4. As it can be seen, MMSM was also successful in exploring the design space and attaining more appropriate design regarding the weight. Search of the design space was more accurate and more comprehensive.

4.3 A 160-bar power transmission tower

In this example, the 160-bar power transmission tower shown in Fig. 8 is optimized.

Nodal coordinates of the 160-bar power transmission tower are defined in Table 5. Here, E and ρ for the structural members are considered as 2.047 x 10^6 kgf/cm^2 and 0.00785 kg/cm^3, respectively.

Members of the 160-bar power transmission tower are categorized into 38 groups and optimal design is performed using the sections list (Table 6) based on IS-808 angles [29].

The allowable values of ± 1500 kgf/cm^2 are employed for compressive and tensile stresses, and the buckling stress constraints for the compressive members, based on IS-808 code, are considered as follows [29, 30]:

For $kl/r \leq 120$

$$\sigma_{all} = 1300 - \frac{(kl/r)^2}{24} \tag{37}$$

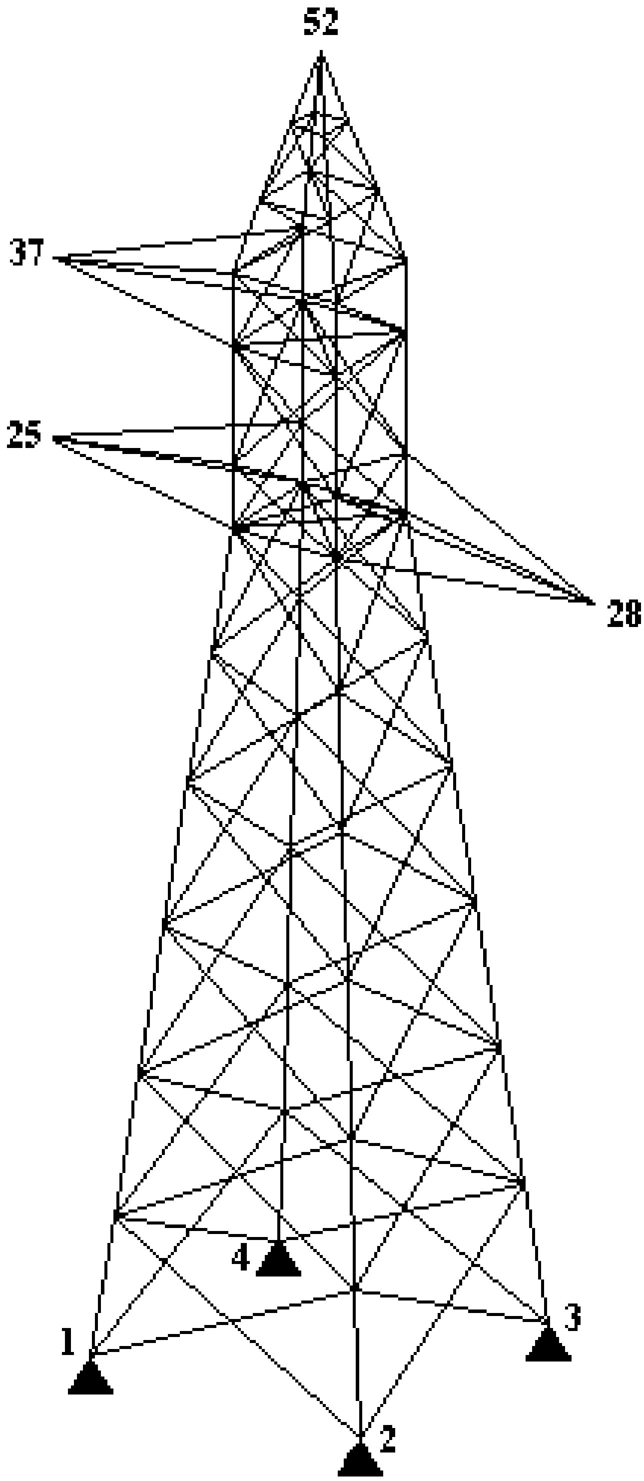

Fig. 8. Schematic of a 160-bar power transmission tower

Tab. 4. Optimal design comparison for the 244-bar power transmission tower

Element group	Toğan [28]	MMSM	Element group	Toğan [28]	MMSM
1	–	L 1 1/4 x 1 1/4 x 3/16	14	–	L 2 x 2 x 1/8
2	–	L 4 x 4 x 3/8	15	–	L 6 x 6 x 3/4
3	–	L 2 1/2 x 2 1/2 x 3/16	16	–	L 4 x 4 x 5/16
4	–	L 4 x 4 x 5/16	17	–	L 2 x 2 x 1/8
5	–	L 3 x 3 x 3/16	18	–	L 2 x 2 x 1/8
6	–	L 5 x 5 x 7/16	19	–	L 2 1/2 x 2 1/2 x 3/16
7	–	L 1 1/4 x 1 1/4 x 3/16	20	–	L 5 x 5 x 7/8
8	–	L 6 x 6 x 3/8	21	–	L 3 1/2 x 3 1/2 x 1/4
9	–	L 2 1/2 x 2 1/2 x 3/16	22	–	L 2 1/2 x 2 1/2 x 3/16
10	–	L 3 x 3 x 3/16	23	–	L 2 1/2 x 2 1/2 x 3/16
11	–	L 4 x 4 x 7/16	24	–	L 2 x 2 x 1/8
12	–	L 5 x 5 x 3/8	25	–	L 1 1/4 x 1 1/4 x 3/16
13	–	L 2 1/2 x 2 1/2 x 3/16	26	–	L 1 1/4 x 1 1/4 x 3/16
Volume		**920050 cm^3**			**757637.35 cm^3**

Tab. 5. Nodal coordinates of the 160-bar power transmission tower

No	X - *cm*	Y - *cm*	Z - *cm*	No	X - *cm*	Y - *cm*	Z - *cm*	No	X - *cm*	Y - *cm*	Z - *cm*
1	−105.000	−105.000	0.000	19	60.085	60.085	710.000	37	−207.000	0.000	1256.500
2	105.000	−105.000	0.000	20	−60.085	60.085	710.000	38	40.000	40.000	1256.500
3	105.000	105.000	0.000	21	−49.805	−49.805	872.500	39	−40.000	40.000	1256.500
4	−105.000	105.000	0.000	22	49.805	−49.805	872.500	40	−40.000	−40.000	1346.500
5	−93.929	−93.929	175.000	23	49.805	49.805	872.500	41	40.000	−40.000	1346.500
6	93.929	−93.929	175.000	24	−49.805	49.805	872.500	42	40.000	40.000	1346.500
7	93.929	93.929	175.000	25	−214.000	0.000	1027.500	43	−40.000	40.000	1346.500
8	−93.929	93.929	175.000	26	−40.000	−40.000	1027.500	44	−26.592	−26.592	1436.500
9	−82.859	−82.859	350.000	27	40.000	−40.000	1027.500	45	26.592	−26.592	1436.500
10	82.859	−82.859	350.000	28	214.000	0.000	1027.500	46	26.592	26.592	1436.500
11	82.859	82.859	350.000	29	40.000	40.000	1027.500	47	−26.592	26.592	1436.500
12	−82.859	82.859	350.000	30	−40.000	40.000	1027.500	48	−12.737	−12.737	1526.500
13	−71.156	−71.156	535.000	31	−40.000	−40.000	1105.500	49	12.737	−12.737	1526.500
14	71.156	−71.156	535.000	32	40.000	−40.000	1105.500	50	12.737	12.737	1526.500
15	71.156	71.156	535.000	33	40.000	40.000	1105.500	51	−12.737	12.737	1526.500
16	−71.156	71.156	535.000	34	−40.000	40.000	1105.500	52	0.000	0.000	1615.000
17	−60.085	−60.085	710.000	35	−40.000	−40.000	1256.500				
18	60.085	−60.085	710.000	36	40.000	−40.000	1256.500				

And if $kl/r > 120$, then

$$\sigma_{all} = \frac{10^7}{(kl/r)^2} \tag{38}$$

where$l$ is length of the member, r is the radius of gyration and$k$ is the effective length factor. For this steel tower, k is assumed to be 1.0 [29, 30].

This steel tower is subjected to eight loading conditions as shown in Table 7.

Fig. 9 demonstrates the convergence trend graph for the average of 10 MMSM performances with the best optimization process for 160-bar power transmission tower.

Optimal design resulting from the MMSM and also the results from other references are presented in Table 8. The resulting convergence trend graph and optimal design indicate acceptable suitable performance of the MMSM.

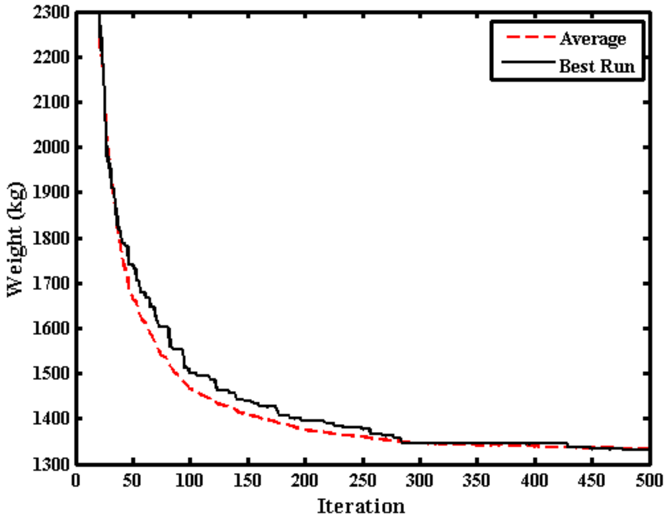

Fig. 9. The convergence history for the 160-bar power transmission tower

Tab. 6. Available cross-sections for the 160-bar power transmission tower

No.	A - cm^2	r - cm	No.	A - cm^2	r - cm	No.	A - cm^2	r - cm
1	1.84	0.47	15	9.40	1.35	29	33.90	2.33
2	2.26	0.57	16	10.47	1.36	30	34.77	2.97
3	2.66	0.67	17	11.38	1.45	31	39.16	2.54
4	3.07	0.77	18	12.21	1.55	32	43.00	2.93
5	3.47	0.87	19	13.79	1.76	33	45.65	2.94
6	3.88	0.97	20	15.39	1.95	34	46.94	2.94
7	4.79	0.97	21	17.03	1.74	35	51.00	2.92
8	5.27	1.06	22	19.03	1.94	36	52.10	3.54
9	5.75	1.16	23	21.12	2.16	37	61.82	3.96
10	6.25	1.26	24	23.20	2.36	38	61.90	3.52
11	6.84	1.15	25	25.12	2.57	39	68.30	3.51
12	7.44	1.26	26	27.50	2.35	40	76.38	3.93
13	8.06	1.36	27	29.88	2.56	41	90.60	3.92
14	8.66	1.46	28	32.76	2.14	42	94.13	3.92

Tab. 7. Load cases for the 160-bar power transmission tower

Loading conditions	Joint number	X - kgf	Y - kgf	Z - kgf	Loading conditions	Joint number	X - kgf	Y - kgf	Z - kgf
1	25	−1091	–	−546	5	25	−1015	–	−546
	28	−1091	–	−546		28	−636	1259	−428
	37	−996	–	−546		37	−951	–	−546
	52	−868	–	−491		52	−917	–	−491
2	25	−1091	–	−546	6	25	−1015	–	−546
	28	−1091	–	−546		28	−1015	–	−546
	37	−996	–	−546		37	−572	1303	−428
	52	−493	1245	−363		52	−917	–	−491
3	25	−1015	–	−546	7	25	−1015	–	−546
	28	−1015	–	−546		28	−636	1303	-428
	37	−951	–	−546		37	−951	–	−546
	52	−917	–	−491		52	−917	–	−491
4	25	−1015	–	−546	8	25	−1015	–	−546
	28	−1015	–	−546		28	−1015	–	−546
	37	−572	1259	−428		37	−951	–	−546
	52	−917	–	−546		52	−498	1460	−363

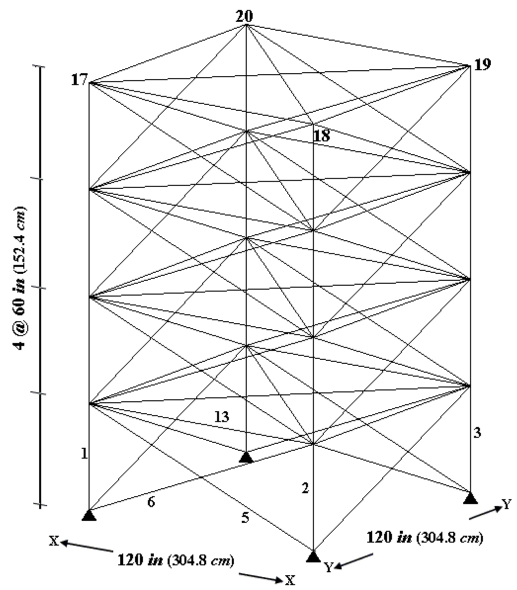

Fig. 10. Schematic of a 72-bar steel tower

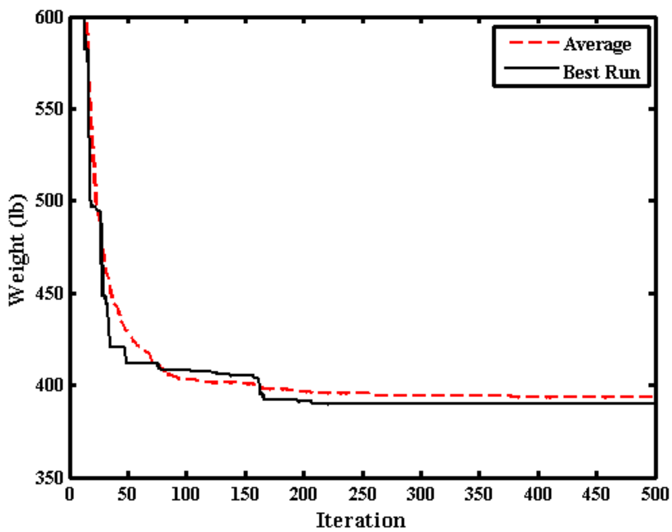

Fig. 11. The convergence history for the 72-bar steel tower

Tab. 8. Optimal design comparison for the 160-bar power transmission tower

Element group	[30]	[27]	[29]	MMSM	Element group	[30]	[27]	[29]	MMSM
1	19.03	19.03	19.03	19.03	20	3.07	3.07	3.07	3.07
2	5.27	5.27	5.27	5.27	21	2.66	3.07	3.07	2.66
3	19.03	19.03	19.03	19.03	22	8.06	8.66	8.06	8.06
4	5.27	5.27	5.27	5.27	23	5.27	5.75	5.27	5.27
5	19.03	19.03	19.03	19.03	24	7.44	6.25	6.25	6.25
6	5.75	5.75	5.75	5.75	25	6.25	5.75	5.75	5.75
7	17.03	15.39	15.39	15.39	26	1.84	1.84	1.84	1.84
8	6.25	5.75	5.75	5.75	27	4.79	4.79	4.79	4.79
9	13.79	13.79	13.79	13.79	28	2.66	2.66	2.66	2.66
10	6.25	5.75	5.75	5.75	29	3.47	3.47	3.47	3.47
11	5.75	5.75	5.75	5.75	30	1.84	1.84	1.84	1.84
12	12.21	12.21	12.21	12.21	31	2.26	2.26	2.26	2.26
13	6.84	6.25	6.25	6.25	32	3.88	3.88	3.88	3.88
14	5.75	5.75	5.75	5.75	33	1.84	1.84	1.84	1.84
15	2.66	3.47	2.66	2.66	34	1.84	2.26	1.84	1.84
16	7.44	7.44	7.44	7.44	35	3.88	3.88	3.88	3.88
17	1.84	1.84	1.84	1.84	36	1.84	1.84	1.84	1.84
18	8.66	9.40	8.66	8.66	37	1.84	1.84	3.47	1.84
19	2.66	2.66	2.66	2.66	38	3.88	3.88	3.88	3.88
Weight (*kg*)						**1359.781**	**1336.7493**	**1331.75**	**1329.715**

Tab. 9. Load case for the 72-bar steel tower

Loading conditions	Joint number	P_X - *Kips* (*kN*)	P_y - *Kips* (*kN*)	P_z - *Kips* (*kN*)
1	17	5.0 (22.241)	5.0 (22.241)	−5.0 (−22.241)
	18	–	–	–
	19	–	–	–
	20	–	–	–
2	17	–	–	−5.0 (−22.241)
	18	–	–	−5.0 (−22.241)
	19	–	–	−5.0 (−22.241)
	20	–	–	−5.0 (−22.241)

4.4 A 72-bar steel tower

As the last example, the optimization of a 72-bar steel tower, shown in Fig. 10, is considered.

For the present structure, E and ρ are considered as 10000 *ksi* (68947.6 *MPa*) and 0.1 lb/in^2 (2767.99 kg/m^3), respectively. Stress range for the truss members and the maximum nodal displacement are limited to ±25 *ksi* (±172.369 *MPa*) and ±0.25 *in* (0.635 *cm*), respectively. Present tower members are categorized into 16 groups. Table 9 shows the applied loads to the structures in two different conditions.

Available sections list is presented in Table 10.

Following the optimization process based on the MMSM for 72-bar steel tower, convergence trend is obtained as depicted in Fig. 11. Similar to the previous examples, in this figure, the average of 10 independent and consecutive runs and the best results base on MMSM method are plotted. In this example, these two graphs are close to each other. Results from the optimal design based on MMSM in comparison to those of the other references are presented in Table 11.

5 Conclusions

- By applying island distribution in the proposed MMSM algorithm, resulting responses show great diversity, and design space is explored to greater extent. The reason for this is associated with different metaheuristic algorithms allocated to the islands. Thus, design space is explored intelligently and the chance of being trapped in local optimum has decreased, while the possibility of obtaining overall optimum is increased.
- Using MMSM leads to the simultaneous use of several meta-heuristic methods, and thus all advantageous of meta-heuristic algorithms are incorporated in the framework of one optimization algorithm.
- In meta-heuristic algorithms, due to the effect of parameters and governing relations on the results, subsequent executions are used in which the amount of parameters are changed to obtain better answers. Although, due to the relative parameter independence of the MMSM, this algorithm is free of subsequent executions for avoiding to be trapped in local optima. Therefore, MMSM moves to global optimum with a reliable

Tab. 10. Available cross-sections for the 72-bar steel tower

No.	$in^2(mm^2)$	No.	$in^2(mm^2)$	No.	$in^2(mm^2)$	No.	$in^2(mm^2)$
1	0.111 (71.613)	17	1.563 (1008.385)	33	3.840 (2477.414)	49	11.500 (7419.430)
2	0.141 (90.968)	18	1.620 (1045.159)	34	3.870 (2496.769)	50	13.500 (8709.660)
3	0.196 (126.451)	19	1.800 (1161.288)	35	3.880 (2503.221)	51	13.900 (8967.724)
4	0.250 (161.290)	20	1.990 (1283.868)	36	4.180 (2696.769)	52	14.200 (9161.272)
5	0.307 (198.064)	21	2.130 (1374.191)	37	4.220 (2722.575)	53	15.500 (9999.980)
6	0.391 (252.258)	22	2.380 (1535.481)	38	4.490 (2896.768)	54	16.000 (10322.560)
7	0.442 (285.161)	23	2.620 (1690.319)	39	4.590 (2961.284)	55	16.900 (10903.204)
8	0.563 (363.225)	24	2.630 (1696.771)	40	4.800 (3096.768)	56	18.800 (12129.008)
9	0.602 (388.386)	25	2.880 (1858.061)	41	4.970 (3206.445)	57	19.900 (12838.684)
10	0.766 (494.193)	26	2.930 (1890.319)	42	5.120 (3303.219)	58	22.000 (14193.520)
11	0.785 (506.451)	27	3.090 (1993.544)	43	5.740 (3703.218)	59	22.900 (14774.164)
12	0.994 (641.289)	28	1.130 (729.031)	44	7.220 (4658.055)	60	24.500 (15806.420)
13	1.000 (645.160)	29	3.380 (2180.641)	45	7.970 (5141.925)	61	26.500 (17096.740)
14	1.228 (792.256)	30	3.470 (2238.705)	46	8.530 (5503.215)	62	28.000 (18064.480)
15	1.266 (816.773)	31	3.550 (2290.318)	47	9.300 (5999.988)	63	30.000 (19354.800)
16	1.457 (939.998)	32	3.630 (2341.931)	48	10.850 (6999.986)	64	33.500 (21612.860)

Tab. 11. Optimal design comparison for the 72-bar steel tower

Members	Optimal cross-sectional area - in^2 (mm^2)						
	[31]	[15]	[32]	[18]	[33]	[34]	MMSM
A_1-A_4	0.196 (126.451)	1.800 (1161.288)	1.990 (1283.868)	1.990 (1283.868)	1.563 (1008.385)	1.800 (1161.288)	1.990 (1283.868)
A_5-A_{12}	0.602 (388.386)	0.442 (285.161)	0.442 (285.161)	0.602 (388.386)	0.563 (363.225)	0.563 (363.225)	0.442 (285.161)
A_{13}-A_{16}	0.307 (198.064)	0.141 (90.968)	0.111 (71.613)	0.111 (71.613)	0.111 (71.613)	0.111 (71.613)	0.111 (71.613)
A_{17}-A_{18}	0.766 (494.193)	0.111 (71.613)	0.111 (71.613)	0.111 (71.613)	0.111 (71.613)	0.111 (71.613)	0.111 (71.613)
A_{19}-A_{22}	0.391 (252.258)	1.228 (792.256)	0.994 (641.289)	1.266 (816.773)	1.266 (816.773)	1.266 (816.773)	1.266 (816.773)
A_{23}-A_{30}	0.391 (252.258)	0.563 (363.225)	0.563 (363.225)	0.442 (285.161)	0.563 (363.225)	0.563 (363.225)	0.563 (363.225)
A_{31}-A_{34}	0.141 (90.968)	0.111 (71.613)	0.111 (71.613)	0.111 (71.613)	0.111 (71.613)	0.111 (71.613)	0.111 (71.613)
A_{35}-A_{36}	0.111 (71.613)	0.111 (71.613)	0.111 (71.613)	0.111 (71.613)	0.111 (71.613)	0.111 (71.613)	0.111 (71.613)
A_{37}-A_{40}	1.800 (1161.288)	0.563 (363.225)	0.563 (363.225)	0.442 (285.161)	0.391 (252.258)	0.563 (363.225)	0.442 (285.161)
A_{41}-A_{48}	0.602 (388.386)	0.563 (363.225)	0.563 (363.225)	0.602 (388.386)	0.563 (363.225)	0.442 (285.161)	0.563 (363.225)
A_{49}-A_{52}	0.141 (90.968)	0.111 (71.613)	0.111 (71.613)	0.111 (71.613)	0.111 (71.613)	0.111 (71.613)	0.111 (71.613)
A_{53}-A_{54}	0.307 (198.064)	0.250 (161.290)	0.111 (71.613)	0.111 (71.613)	0.111 (71.613)	0.111 (71.613)	0.141 (90.968)
A_{55}-A_{58}	1.563 (1008.385)	0.196 (126.451)	0.196 (126.451)	0.196 (126.451)	0.196 (126.451)	0.196 (126.451)	0.196 (126.451)
A_{59}-A_{66}	0.766 (494.193)	0.563 (363.225)	0.563 (363.225)	0.563 (363.225)	0.563 (363.225)	0.602 (388.386)	0.563 (363.225)
A_{67}-A_{70}	0.141 (90.968)	0.442 (285.161)	0.442 (285.161)	0.391 (252.258)	0.391 (252.258)	0.391 (252.258)	0.391 (252.258)
A_{71}-A_{72}	0.111 (71.613)	0.563 (363.225)	0.766 (494.193)	0.442 (285.161)	0.602 (388.386)	0.563 (363.225)	0.602 (388.386)
Weight *lb* – (*kg*)	**427.203 (193.776)**	**393.380 (178.434)**	**393.05 (178.284)**	**391.607 (177.63)**	**390.18 (176.983)**	**389.87 (176.842)**	**389.684 (176.758)**

rate, and the probability of getting trapped in local optimum is reduced.

- Since in the first variant of the proposed algorithm (MMSM 1), best members of each island are transferred to other islands during migration process, or in the second variant (MMSM 2) bests members are transferred to the selected island and substituted with the members of lower fitnesses, it is anticipated that the convergence speed and average growth rate of the population fitness to be enhanced.

Acknowledgments

The authors would thank the authors of Ref. [28] for providing the design data of the 244-bar transmission tower.

References

1 **Fogel L J, Qwens A J, Walsh M J**, *Artificial Intelligence Through Simulated Evolution*, John Wiley & Sons, 1966.

2 **Goldberg D E**, *Genetic Algorithms in Search Optimization and Machine Learning*, Addison-Wesley, 1989.

3 **Kirkpatrick S, Gelatt C D, Vecchi M P**, *Optimization by Simulated Annealing*, Science, **220**(4598), (1983), 671–680, DOI 10.1126/science.220.4598.671.

4 **Glover F**, *Future paths for integer programming and links to artificial intelligence*, Computers & Operations Research, **13**(5), (1986), 533–549, DOI 10.1016/0305-0548(86)90048-1.

5 **Colorni A, Dorigo M, Maniezzo V**, *Distributed optimization by ant colony*, Proceedings of the First European Conference on Artificial Life, In:, 1991, pp. 134–142.

6 **Kennedy J, Eberhart R C**, *Particle swarm optimization*, Proceedings of IEEE, International of Conference on Neural Networks, In:, 1995, pp. 1942–1948.

7 **Geem Z W, Kim J H, Loganathan G V**, *A New Heuristic Optimization Algorithm: Harmony Search*, SIMULATION, **76**(2), (2001), 60–68, DOI 10.1177/003754970107600201.

8 **Erol O K, Eksin I**, *A new optimization method: Big Bang–Big Crunch*, Advances in Engineering Software, **37**(2), (2006), 106–111, DOI 10.1016/j.advengsoft.2005.04.005.

9 **Rashedi E, Nezamabadi-pour H, Saryazdi S**, *GSA: A Gravitational Search Algorithm*, Information Sciences, **179**(13), (2009), 2232–2248, DOI 10.1016/j.ins.2009.03.004.

10 **Kaveh A, Talatahari S**, *A novel heuristic optimization method: charged system search*, Acta Mechanica, **213**(3-4), (2010), 267–289, DOI 10.1007/s00707-009-0270-4.

11 **Kaveh A, Khayatazad M**, *A new meta-heuristic method: Ray Optimization*, Computers & Structures, **112-113**, (2012), 283–294, DOI 10.1016/j.compstruc.2012.09.003.

12 **Kaveh A**, *Advances in Metaheuristic Algorithms for Optimal Design of Structures*, Springer, 2014, DOI 10.1007/978-3-319-05549-7.

13 **Dede T, Bekiroğlu S, Ayvaz Y**, *Weight minimization of trusses with genetic algorithm*, Applied Soft Computing, **11**(2), (2011), 2565–2575, DOI 10.1016/j.asoc.2010.10.006.

14 **Degertekin S O**, *Improved harmony search algorithms for sizing optimization of truss structures*, Computers & Structures, **92-93**, (2012), 229–241, DOI 10.1016/j.compstruc.2011.10.022.

15 **Kaveh A, Talatahari S**, *A particle swarm ant colony optimization for truss structures with discrete variables*, Journal of Constructional Steel Research, **65**(8–9), (2009), 1558–1568, DOI 10.1016/j.jcsr.2009.04.021.

16 **Kaveh A, Talatahari S**, *Particle swarm optimizer, ant colony strategy and harmony search scheme hybridized for optimization of truss structures*, Computers & Structures, **87**(5–6), (2009), 267–283, DOI 10.1016/j.compstruc.2009.01.003.

17 **Kao Y T, Zahara E**, *A hybrid genetic algorithm and particle swarm optimization for multimodal functions*, Applied Soft Computing, **8**(2), (2008), 849–857, DOI 10.1016/j.asoc.2007.07.002.

18 **Kalatjari V R, Talebpour M H**, *Sizing and topology optimization of truss structures by modified multi-search method*, Journal of Civil and Surveying Engineering, **45**(3), (2011), 351–363.

19 **Izzo D, Rucínski M, Ampatzis C**, *Parallel global optimisation metaheuristics using an asynchronous island-model*, Proceedings of IEEE Congress on Evolutionary Computation. Trondheim, Norway, In:, 2009, pp. 2301–2308.

20 **Kaveh A, Kalatjari V R, Talebpour M H, Torkamanzadeh J**, *Configuration optimization of trusses using a multi heuristic based search method*, International Journal of Optimization in Civil Engineering, **3**(1), (2013), 151–178.

21 *Design of Latticed Steel Transmission Structures*, American Society of civil engineering (ASCE 10-97); Chicago (IL), 2000.

22 *TIA/EIA STANDARD, Structural standard for steel antenna towers and antenna supporting structures, TIA/EIA-222-F*, Telecommunications industry association; Arlington, USA, 1996.

23 *Manual of steel construction-allowable stress design*, 9th, American Institute of Steel Construction (AISC); Chicago (IL), 1998.

24 **Hasançebi O, Çarbaş S, Doğan E, Erdal F, Saka M P**, *Performance evaluation of metaheuristic search techniques in the optimum design of real size pin jointed structures*, Computers & Structures, **87**(5-6), (2009), 284–302, DOI 10.1016/j.compstruc.2009.01.002.

25 **Lee K S, Geem Z W, Lee S-h, Bae K-wo**, *The harmony search heuristic algorithm for discrete structural optimization*, Engineering Optimization, **37**(7), (2005), 663–684, DOI 10.1080/03052150500211895.

26 **Kaveh A, Talatahari S**, *Optimal design of skeletal structures via the charged system search algorithm*, Structural and Multidisciplinary Optimization, **41**(6), (2010), 893–911, DOI 10.1007/s00158-009-0462-5.

27 **Capriles P V S Z, Fonseca L G, Barbosa H J C, Lemonge A C C**, *Rank-based ant colony algorithms for truss weight minimization with discrete variables*, Communications in Numerical Methods in Engineering, **23**(6), (2006), 553–575, DOI 10.1002/cnm.912.

28 **Toğan V, Daloğlu A T**, *Optimization of 3d trusses with adaptive approach in genetic algorithms*, Engineering Structures, **28**(7), (2006), 1019–1027, DOI 10.1016/j.engstruct.2005.11.007.

29 **Juang D S, Chang W T**, *A revised discrete Lagrangian-based search algorithm for the optimal design of skeletal structures using available sections*, Structural and Multidisciplinary Optimization, **31**(3), (2006), 201–210, DOI 10.1007/s00158-005-0571-8.

30 **Groenwold A A, Stander N**, *Optimal discrete sizing of truss structures subject to buckling constraints*, Structural Optimization, **14**(2-3), (1997), 71–80, DOI 10.1007/BF01812508.

31 **Wu S-J, Chow P-T**, *Steady-state genetic algorithms for discrete optimization of trusses*, Computers & Structures, **56**(6), (1995), 979–991, DOI 10.1016/0045-7949(94)00551-D.

32 **Kaveh A, Talatahri S**, *A charged system search with a fly to boundary method for discrete optimum design of truss structures*, Asian Journal of Civil Engineering (Building and Housing), **11**(3), (2010), 277–293.

33 **Kaveh A, Kalatjari V R, Talebpour M H**, *Optimization of skeletal structures using a hybridized ACO, HS and GA algorithm*, Iranian Journal of Science and Technology, Transaction of Civil Engineering, **38**, (2014), 1–20.

34 **Kaveh A, Bakhshpoori T**, *Optimum design of space trusses using cuckoo search algorithm with levy flights*, Iranian Journal of Science and Technology, Transaction of Civil Engineering, **37**(C1), (2013), 1–15.